

University of Groningen

Numerical method to compute hypha tip growth for data driven validation

De Jong, T. G.; Sterk, A. E.; Guo, F.

Published in:
IEEE Access

DOI:
[10.1109/ACCESS.2019.2912638](https://doi.org/10.1109/ACCESS.2019.2912638)

IMPORTANT NOTE: You are advised to consult the publisher's version (publisher's PDF) if you wish to cite from it. Please check the document version below.

Document Version
Publisher's PDF, also known as Version of record

Publication date:
2019

[Link to publication in University of Groningen/UMCG research database](#)

Citation for published version (APA):

De Jong, T. G., Sterk, A. E., & Guo, F. (2019). Numerical method to compute hypha tip growth for data driven validation. *IEEE Access*, 7, 53766-53776. <https://doi.org/10.1109/ACCESS.2019.2912638>

Copyright

Other than for strictly personal use, it is not permitted to download or to forward/distribute the text or part of it without the consent of the author(s) and/or copyright holder(s), unless the work is under an open content license (like Creative Commons).

Take-down policy

If you believe that this document breaches copyright please contact us providing details, and we will remove access to the work immediately and investigate your claim.

Downloaded from the University of Groningen/UMCG research database (Pure): <http://www.rug.nl/research/portal>. For technical reasons the number of authors shown on this cover page is limited to 10 maximum.

Received March 26, 2019, accepted April 15, 2019, date of publication April 24, 2019, date of current version May 3, 2019.

Digital Object Identifier 10.1109/ACCESS.2019.2912638

Numerical Method to Compute Hypha Tip Growth for Data Driven Validation

THOMAS G. DE JONG¹, ALEF E. STERK¹, AND FENG GUO²

¹Bernoulli Institute, University of Groningen, 9700 AK Groningen, The Netherlands

²School of Information Science and Engineering, Xiamen University, Xiamen 361005, China

Corresponding author: Thomas G. de Jong (t.g.de.jong.math@gmail.com)

This work was supported in part by the Ph.D. Grant of the Nederlandse Organisatie voor Wetenschappelijk Onderzoek (NWO) Cluster Nonlinear Dynamics in Natural Systems (NDNS+), in part by the NWO Vici under Grant 639.033.008, and in part by the National Key R&D Program under Grant 2017YFC0113000 and Grant 2016YFB1001503.

ABSTRACT Hyphae are fungal filaments that can occur in both pathogenic and symbiotic fungi. Consequently, it is important to understand what drives the growth of hyphae. A single hypha cell grows by localized cell extension at their tips. This type of growth is referred to as tip growth. The interconnection between different biological components driving the tip growth is not fully understood. Consequently, many theoretical models have been formulated. It is important to develop methods, such that these theoretical models can be validated using experimentally obtained data. In this paper, we consider the Ballistic Ageing Thin viscous Sheet (BATS) model by Prokert, Hulshof, and de Jong (2019). The governing equations of the BATS model are given by ordinary differential equations that depend on a function called the viscosity function. We present a numerical method for computing solutions of the governing equations that resemble the tip growth. These solutions can be compared to experimental data to validate the BATS model. Since the authors are unaware of the existence of the required data to validate this model, a variety of theoretical scenarios were considered. Our numerical results suggest that if there exists a solution that corresponds to the tip growth, then there exists a one-parameter family of solutions corresponding to the tip growth.

INDEX TERMS Bifurcation, biomechanics, cells (biology), differential equations, morphogenesis, Newton method, nonlinear equations, numerical analysis, shooting method, tip growth.

I. INTRODUCTION

Filamentous pathogenic fungi commonly occur as respiratory infections in immune-compromised patients [5]. They can also produce a wide variety of beneficial drugs and antibiotics [16]. More recently, studies indicate that filamentous fungi are useful in degrading pharmaceuticals [18]. As more pharmaceuticals enter the ecosystem through livestock rearing this might remedy the negative effects of pharmaceuticals on fauna and human health. In nature filamentous fungi play an important role in decomposing organisms. Fungi convert dead cells into soluble compounds that can be absorbed by plants. Consequently, it is important to understand what drives the growth of fungal filaments [11].

Fungal filaments are called hyphae. Hyphae grow by localized cell extension at their tips. Hence, this growth

phenomenon is called tip growth. During tip growth a hypha cell exhibits extreme lengthwise growth while its shape remains qualitatively the same and the tip's velocity remains approximately constant. Furthermore, in the absence of spatial influences the cell's shape is almost rotationally symmetric. In Fig. 1 we display an idealized cell wall shape during tip growth at equally spaced time steps t_0 .

The interconnection between different biological components driving tip growth is not fully understood. Consequently, many theoretical models have been formulated [2]–[4], [7]–[9]. The model of Bartnicki-Garcia and Gierz [2] and Bartnicki-Garcia *et al.* [3] gives a detailed description of the internal transport of new cell wall building material. The model of Campàs and Mahadevan [4] gives a detailed description of the cell wall evolution. To obtain an improved model the models of Bartnicki-Garcia *et al.* and Campàs, Mahadevan were combined in [12]. This new model is called the Ballistic Ageing Thin viscous Sheet (BATS) model. The governing equations are given by an ordinary

The associate editor coordinating the review of this manuscript and approving it for publication was Yonghong Peng.




Cell shape	Time
	$t = 0$
	$t = t_0$
	$t = 2t_0$

FIGURE 1. Qualitative description of hypha tip growth.

differential equation which is dependent on an experimentally determined function called the viscosity function. This model was not validated using experimental data. Since there exists a lot of variety between fungal hypha species it is important to first construct a method which can validate the model given processed experimental data. In this paper we present a numerical method which, for suitable viscosity functions, can compute solutions of the BATS model which resemble hypha tip growth. Furthermore, we give numerical evidence that for certain viscosity functions there exist no solutions that resemble tip growth.

Solutions of the governing ODE which resemble tip growth cannot be straightforwardly computed using a standard ODE solver since the majority of solutions of the ODE do not resemble tip growth. By studying the limiting properties at the tip and the base of the cell we can restrict to a family of solutions. The solutions satisfying the limiting properties at the tip admit a classification which allows us to specify which solutions do not resemble tip growth. Using a Newton method we can then connect the remaining solutions to solutions satisfying the limiting base properties.

Let us give an overview of this paper. In Section II we revise the BATS model. In Section III we present the numerical method for computing solutions corresponding to tip growth. This method relies on computing expansions, defining a classification of solutions and a shooting method based on a Newton method. In Section IV we apply the method to a variety of viscosity functions. The numerical results suggest that viscosity functions exist which admit solutions corresponding to hypha tip growth. In addition, the numerical results suggest that there also exist viscosity functions which do not admit the existence of solutions corresponding to hypha tip growth. Finally, in Section V we present conclusions and topics for future work.

II. BALLISTIC AGEING THIN VISCOUS SHEET MODEL

The BATS model is based on the thin viscous sheet tip growth model of Campàs and Mahadevan [4] and the ballistic tip growth model of Bartnicki-Garcia and Gierz [2]

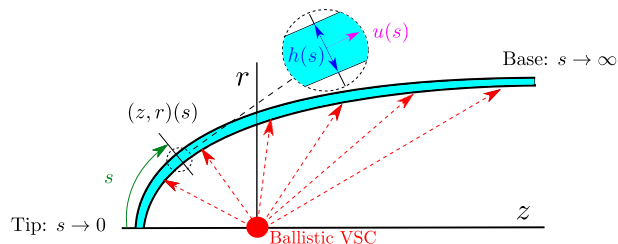


FIGURE 2. Overview of the BATS model.

and Bartnicki-Garcia *et al.* [3]. It connects these two models by introducing a so-called age equation. In this section we will briefly revise the BATS model and present the governing equations. The details can be found in [12]. For a short biomechanical overview of the BATS model we refer to [13]. For more details concerning the biology of hypha growth we refer to [1], [6], [8], [10], [14], [17], [19].

A. MODELLING TIP GROWTH

We assume that the cell wall shape is axially symmetric. Thus, at a fixed time we describe the cell shape in cylindrical variables (z, r, ϕ) . Due to its axial symmetry the cell shape can be fully described in the (z, r) -plane. We parameterize the r, z variables by s , the arclength to the tip.

During tip growth the cell grows with constant speed in the direction normal to the tip. In addition, the hypha cell preserves its overall shape. Hence, tip growth corresponds to a travelling wave profile: $(z(s) + ct, r(s), \phi)$ with c the travelling wave velocity. We will take $c < 0$.

We consider a moving reference frame where the tip of the cell is fixed at $\lim_{s \rightarrow 0}(z, r) = (z_0, 0)$ with $z_0 < 0$. Note that this removes the dependency on time. We assume that the cell wall is a thin viscous sheet. We assume that the sheet is infinitely long. The base of cell then corresponds to $s \rightarrow \infty$. The sheet is subject to an outward force resulting from the pressure difference. In the hypha biology this corresponds to the pressure difference between the turgor and the atmospheric pressure. At s the thickness of the thin viscous sheet is denoted by $h(s)$ and the tangential velocity is denoted by $u(s)$, see Fig. 2. The travelling wave velocity can then be retrieved by computing $\lim_{s \rightarrow \infty} u(s)$.

Cell wall building material is transported to the cell wall in straight trajectories from an isotropic point source, called the ballistic Vesicle Supply Center (VSC), see Fig. 2. We fix the ballistic VSC at $(z, r) = (0, 0)$. For an alternative model for cell wall building material transport see [15], [20].

We assume that the cell wall ages. The ageing starts when a cell wall building particle is absorbed by the cell wall. Hence, we compute the average age of all cell wall particles at s . Denote by $T(\zeta, s)$ the time it takes a particle in the cell wall to travel from ζ to s . Observe that the tangential velocity, $u(s)$, is parameterized by s . Hence, we have that

$$T(\zeta, s) = \int_{\zeta}^s \frac{1}{u(\sigma)} d\sigma. \tag{1}$$

In Fig. 3 the components of $T(\zeta, s)$ are displayed. There exist other methods to define the local age of the cell wall, for example see [7].

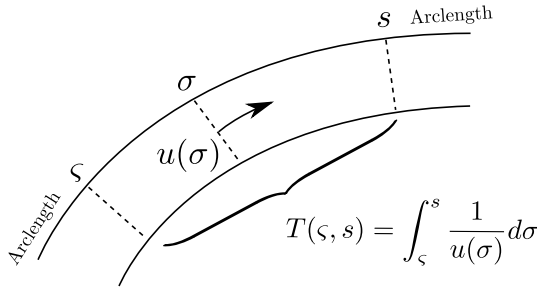


FIGURE 3. Travel time of particles through the cell wall.

We define the cumulative flux $G(s)$ as the total flux of material over the surface of revolution given by the arc from the tip to $\zeta = s$, see Fig. 4.

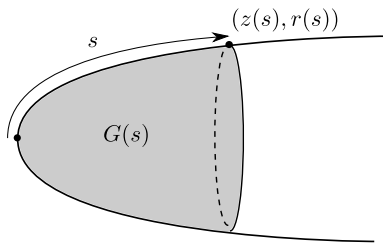


FIGURE 4. $G(s)$ is the total flux through the grey cap.

Observe that since no particles exit the cell wall the flux is equal to the inflow of cell wall building particles. At a point with arclength s there is cell wall material which originally entered at $\zeta \in (0, s)$ and has been part of the cell wall for $T(\zeta, s)$. Weighing $T(\zeta, s)$ by the mass which enters the cell wall at the boundary of the disk at ζ we get $T(\zeta, s)G'(\zeta)$. To obtain the average age we integrate $T(\zeta, s)G'(\zeta)$ over an arc $(0, s)$ and divide it by the total flux over that arc:

$$\Psi(s) = \frac{\int_0^s G'(\zeta)T(\zeta, s)d\zeta}{G(s)}. \tag{2}$$

The integral equation (2) can be reformulated as a differential equation which will be presented in the next section.

We assume that the viscosity depends on age. Hence, the viscosity at s is given by $\mu(\Psi(s))$, where $\mu \in C^\infty(\mathbb{R}_+)$ is the viscosity function. The biology suggests that the cell wall ‘hardens’ with age. In this model ‘hardening’ of the cell wall means that the cell wall’s viscosity increases. Therefore, we require that μ satisfies:

$$\frac{d\mu}{d\Psi} > 0. \tag{3}$$

From an application perspective μ needs to be determined experimentally. Hypha cells can have different material properties based the fungal cell species and the physical circumstances of the cell. Hence, we expect that μ is problem specific. Thus, from a theoretical perspective we want to consider μ as general as possible.

B. GOVERNING EQUATIONS: FIVE DIMENSIONAL FIRST ORDER ODE

The modeling assumptions from Section II-A can be expressed as two force balance equations, a mass conservation equation and an age equation. We can eliminate the u -variable as is shown in [12]. After non-dimensionalisation the governing equations can be expressed as the following five dimensional first order ODE:

$$\begin{aligned} \rho' &= \frac{3}{2} \frac{(1-\rho)^2}{r} \left(-1 + \frac{\mu(\Psi)\Gamma(r, z)\rho\sqrt{1-\rho^2}}{r^3} \right), \\ r' &= \rho, \\ h' &= \left(\frac{r\gamma(\rho, r, z)}{\Gamma(r, z)} - \frac{\rho}{2r} - \frac{r^2}{2\mu(\Psi)\Gamma(r, z)\sqrt{1-\rho^2}} \right) h, \\ \Psi' &= \frac{rh}{\Gamma(r, z)} - \frac{r\gamma(\rho, r, z)}{\Gamma(r, z)} \Psi, \\ z' &= \sqrt{1-\rho^2}, \end{aligned} \tag{4}$$

where the prime denotes the s -derivative,

$$\begin{aligned} \gamma(\rho, r, z) &= \frac{r\sqrt{1-\rho^2} - z\rho}{(z^2 + r^2)^{3/2}}, \\ \Gamma(r, z) &= 1 + \frac{z}{\sqrt{r^2 + z^2}}, \end{aligned} \tag{5}$$

and $\mu \in F$ with

$$F := \{\mu \in C^\infty(\mathbb{R}_+) : \mu' > 0, \lim_{\Psi \rightarrow \infty} \mu(\Psi) = \infty\}. \tag{6}$$

A function $\mu \in F$ is referred to as a viscosity function. We will consider the phase space given by

$$M := \{(\rho, r, h, \Psi, z) \in (-1, 1) \times \mathbb{R}_+ \times \mathbb{R}_+ \times \mathbb{R}_+ \times \mathbb{R}\}. \tag{7}$$

In [12] it is shown that the governing ODE (4) does not have any biologically realistic solutions if it does not satisfy $\lim_{\Psi \rightarrow \infty} \mu(\Psi) = \infty$.

For notational convenience we will denote a solution vector of (4) by x . Hence, we have that $x = (\rho, r, h, \Psi, z)$. When necessary we will indicate the dependence of x on μ by writing $x(\cdot; \mu)$.

C. STEADY TIP GROWTH SOLUTIONS

Steady tip growth solutions are solutions of (4) which correspond to fungal tip growth in the phase space. A solution $x := (\rho, r, h, \Psi, z)$ is called a steady tip growth solution if it is a solution of the ODE (4) which satisfies the following four conditions:

T1 Tip limits:

$$\begin{aligned} \lim_{s \rightarrow 0} \rho(s) &= 1, & \lim_{s \rightarrow 0} r(s) &= 0, \\ \lim_{s \rightarrow 0} h(s) &= h_0 > 0, & \lim_{s \rightarrow 0} \Psi(s) &= h_0 z_0^2, \\ \lim_{s \rightarrow 0} z(s) &= z_0 < 0. \end{aligned}$$

Rationale: The limits for ρ, r, h, z follow directly from the cell shape in Fig. 2. Then, after computing leading order asymptotics the limit for Ψ follows.

T2 Analyticity in r^2 : There exists $s_1 > 0$ and $G \in C^\omega((-a, a), \mathbb{R}^4)$ with $a = r(s_1)^2$ such that

$$(\rho, h, \Psi, z)(s) = G(r(s)^2) \quad \forall s \in (0, s_1).$$

Rationale: This condition follows from the axial symmetry and the smoothness at the tip.

T3 Global constraints: For all $s \in \mathbb{R}_+$ the following constraints are satisfied

$$\rho'(s) < 0, \quad \rho(s) > 0.$$

Rationale: If we require that r satisfies $r'(s) > 0$ and $r''(s) < 0$ for all $s \in \mathbb{R}_+$ we obtain the characteristic tip growth cell shape displayed in Fig. 2. We expect that the thickness and the age are positive for all $s \in \mathbb{R}_+$.

T4 Base limits:

$$\begin{aligned} \lim_{s \rightarrow \infty} \rho(s) &= 0, & \lim_{s \rightarrow \infty} r(s) &= r_\infty > 0, \\ \lim_{s \rightarrow \infty} h(s) &= h_\infty > 0, & \lim_{s \rightarrow \infty} \Psi(s) &= \infty, \\ \lim_{s \rightarrow \infty} z(s) &= \infty. \end{aligned}$$

Rationale: We assume that the cell's length is infinite and that the cell's width converges to a constant. We expect that the cell wall thickness converges to a positive constant. For a detailed derivation of T1-T4 we refer to [12].

Solutions which are not steady tip growth solutions are not meaningful from a biological perspective.

Remark:

- In [12] the T4 condition of steady tip growth solutions does not contain $\lim_{s \rightarrow \infty} \Psi(s)$. In [12] it is shown that the T4 condition without $\lim_{s \rightarrow \infty} \Psi(s)$ implies condition T4. Hence, for convenience it has been absorbed in condition T4.

III. COMPUTING STEADY TIP GROWTH SOLUTIONS

Assume that for some viscosity function μ the governing ODE (4) has a steady tip growth solution. Our objective is to compute the steady tip growth solutions. Observe that T1,T2 are local conditions for small arclength s , T3 is a global condition on arclength s and T4 is a local condition for large arclength s . The T1-T4 conditions are displayed in relation to the r, z -variables. T1 and T2 are conditions related to The limits given in T1 and T4 give degrees of freedom since $h_0, z_0, r_\infty, h_\infty$ are not specified. Then, to approximate steady tip growth solutions we can numerically connect solutions satisfying T1,T2 to solutions satisfying T4 by varying the parameters given by the limits. We then only consider a connecting solution which satisfies T4 to obtain a steady tip growth solution. By computing expansions we will see that solutions satisfying T1,T2 from a two parameter family of solutions and that solutions satisfying T4 form a three parameter family of solutions. Observe that for a solution satisfying T4 this means that besides r_∞, h_∞ from T4 there

is another parameter. The solutions satisfying T1,T2 can be classified in such a way that we can identify solutions which do not satisfy T3. The remaining solution can then be connected to the solutions satisfying T4 using the corresponding expansion.

Note that to compute expansions for solutions satisfying the limiting conditions we must make minor assumptions on μ . These assumptions will be specified in the following subsections.

A. TIP EXPANSION

Let x be a solution of the governing ODE satisfying T1. Observe that the vector field corresponding to (4) is not defined on $\lim_{s \rightarrow 0} x(s)$. Consequently, solutions satisfying T1 cannot be computed using a standard solver. Hence, we compute an expansion for solutions satisfying T1 and T2 which is called the tip expansion.

Let $x(\cdot; \mu) := (\rho, r, h, \Psi, z)(\cdot)$ be a solution of the governing ODE (4) that satisfies T1 and T2. We assume that μ is analytic. The solution $x(\cdot; \mu)$ satisfies

$$\lim_{s \rightarrow 0} h(s) = h_0 > 0, \quad \lim_{s \rightarrow 0} z(s) = z_0 < 0, \quad (8)$$

where $(h_0, z_0) \in Y^{\text{tip}}$ with

$$Y^{\text{tip}} := \mathbb{R}_+ \times \mathbb{R}_-. \quad (9)$$

We assume that $x(s; \mu)$ can be written as a formal expansion in s . We denote the i -th coefficient of the expansion with an (i) superscript and a tip subscript, e.g.,

$$r(s) = r_{\text{tip}}^{(0)} + sr_{\text{tip}}^{(1)} + s^2r_{\text{tip}}^{(2)} + O(s^3).$$

The equality $r' = \rho$ in the governing ODE (4) implies that $\rho_{\text{tip}}^{(i)} = (i+1)r_{\text{tip}}^{(i+1)}$ which together with condition T2 implies that

$$h_{\text{tip}}^{(2i+1)} = \Psi_{\text{tip}}^{(2i+1)} = z_{\text{tip}}^{(2i+1)} = r_{\text{tip}}^{(2i)} = 0.$$

Substituting the resulting expansions in the governing ODE (4) and collecting terms of the same order we can compute unique coefficients corresponding to the higher order terms. We refer to these expansions as tip solution expansions. For our numerical work we will use the tip expansion up to 8th order as higher order expansion do not lead to improved results. The coefficients are lengthy. Denote by $Y_\mu^{\text{tip}} \subseteq Y^{\text{tip}}$ the maximal domain on which the coefficients of the corresponding expansion are defined. We have that

$$Y_\mu^{\text{tip}} = \left\{ (h_0, z_0) \in Y^{\text{tip}} : \frac{10}{3} \neq \frac{h_0 z_0^2 \mu'(h_0 z_0^2)}{\mu(h_0 z_0^2)} \right\}. \quad (10)$$

The derivation of (10) and higher order coefficients of the base expansion are presented in Appendix V-A.

The tip expansion gives strong evidence that a family of solutions satisfying T1, T2 can be parameterized by $(h_0, z_0) \in Y_\mu^{\text{tip}}$. Consequently, given μ we denote a solution satisfying T1, T2 with $(h_0, z_0) = \alpha \in Y_\mu^{\text{tip}}$ by $x_\alpha(\cdot; \mu)$.

B. CLASSIFYING TIP SOLUTIONS

We define tip solutions as solutions $x_\alpha(\cdot; \mu) = (\rho_\alpha, r_\alpha, h_\alpha, \Psi_\alpha, z_\alpha)$ for which there exists a $s_1 > 0$ for which

$$\rho'_\alpha(s; \mu) < 0, \quad \rho_\alpha(s; \mu) > 0, \quad \forall s \in (0, s_1). \quad (11)$$

Observe that since steady tip growth solutions satisfy T3 it follows that a steady tip growth solution is also a tip solution.

In terms of the ρ -variable the numerically computed tip solutions resemble the graph in Fig. 5 or the graph in Fig. 6. Fig. 5 is not a steady tip growth solution since ρ changes sign. Fig. 6 is not a steady tip growth solution since ρ' changes sign.

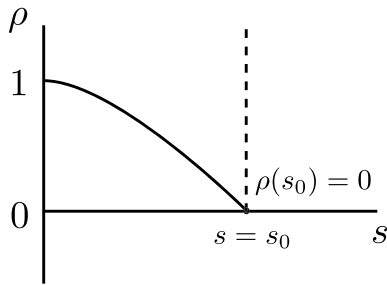


FIGURE 5. The ρ -variable characterizing A_μ .

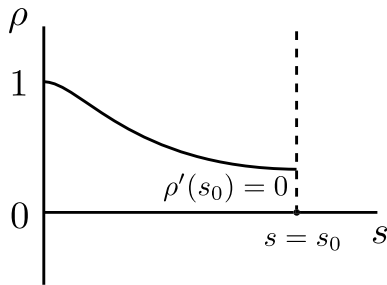


FIGURE 6. The ρ -variable characterizing set B_μ .

Tip continuations The set A_μ and B_μ in Fig. 5 and Fig. 6 are defined by

$$\begin{aligned} A_\mu &:= \{\alpha \in Y_\mu^{\text{tip}} : \exists s_0 \in \mathbb{R}_+, \rho_\alpha(s; \mu)\rho'_\alpha(s; \mu) < 0 \\ &\quad \forall s \in (0, s_0), \rho_\alpha(s_0; \mu) = 0\}, \\ B_\mu &:= \{\alpha \in Y_\mu^{\text{tip}} : \exists s_0 \in \mathbb{R}_+ \rho_\alpha(s; \mu)\rho'_\alpha(s; \mu) < 0, \\ &\quad \forall s \in (0, s_0), \rho'_\alpha(s_0; \mu) = 0\}. \end{aligned} \quad (12)$$

We define

$$X_\mu := Y_\mu^{\text{tip}} \setminus (A_\mu \cup B_\mu). \quad (13)$$

We expect that if steady tip growth solutions exist then they should correspond to tip solutions $x_{\alpha_*}(\cdot; \mu)$ with $\alpha_* \in X_\mu$. The numerical results suggest, as we will see in Section IV-A, that almost all perturbations of $\alpha_* \in X_\mu$ are in $A_\mu \cup B_\mu$. Hence, a tip solution with parameters in X_μ depends sensitively on parameters. Consequently, steady tip growth solutions cannot be approximated by shooting from the tip.

We approximate steady tip growth solutions by connecting the numerically computed tip solutions corresponding to X_μ to an expansion of solutions satisfying T4.

C. BASE EXPANSION

If x is a solution of the governing ODE satisfying T4 then $\lim_{s \rightarrow \infty} \|x(s)\| = \infty$. Consequently, solutions satisfying T4 cannot be computed using a standard solver. Hence, we compute an expansion for solutions satisfying T4 which is called the base expansion.

Let $x(\cdot; \mu) := (\rho, r, h, \Psi, z)(\cdot)$ be a solution of the governing ODE (4) that satisfies condition T4. Then, the solution $x(\cdot; \mu)$ satisfies

$$\lim_{s \rightarrow \infty} h(s) = h_\infty > 0, \quad \lim_{s \rightarrow \infty} r(s) = r_\infty > 0. \quad (14)$$

We assume that $x(s; \mu)$ can be written as a formal expansion in $1/s$. We denote the i -th coefficient of the expansion with an (i) superscript and a base subscript, e.g.,

$$r(s) = r_{\text{base}}^{(0)} + s^{-1}r_{\text{base}}^{(1)} + s^{-2}r_{\text{base}}^{(2)} + O(s^{-3}).$$

We take μ such that v_μ given by

$$v_\mu(\psi) := \begin{cases} 0 & \text{if } \psi = 0, \\ 1/\mu(1/\psi) & \text{otherwise,} \end{cases} \quad (15)$$

is analytic. If $v_\mu(\psi) \sim c_1\psi$ for $\psi \rightarrow 0$ then the formal expansions do not satisfy T4. The proof is given in Appendix VI. If $v_\mu(\psi) = O(\psi^2)$ then from T4 we obtain the following lowest order asymptotics for the converging variables:

$$r_{\text{base}}^{(0)} = r_\infty, \quad h_{\text{base}}^{(0)} = h_\infty. \quad (16)$$

Substituting the resulting expansions in the governing ODE (4) we find that the leading order terms of Ψ, z are of order s . We denote the leading order terms of Ψ and z by $\Psi_{\text{base}}^{(-1)}$ and $z_{\text{base}}^{(-1)}$, respectively. We obtain that

$$\Psi_{\text{base}}^{(-1)} = \frac{r_\infty h_\infty}{2}, \quad z_{\text{base}}^{(-1)} = 1.$$

Substituting the resulting expansions in the governing ODE (4) and collecting terms of the same order we can compute coefficients corresponding to the higher order terms. These coefficients are not uniquely determined given r_∞, h_∞ . More specifically, the zero-th order terms corresponding to the Ψ - and z -component introduce two additional free parameters:

$$\Psi_{\text{base}}^{(0)} = \Psi_c, \quad z_{\text{base}}^{(0)} = z_c. \quad (17)$$

Since $\Psi_{\text{base}}^{(-1)}$ and $z_{\text{base}}^{(-1)}$ are non-zero we can absorb Ψ_c or z_c in the independent variable s . We will fix $z_c = 0$. Observe that (17) implies that T4 is insufficient to define a unique solution.

Let $(r_\infty, h_\infty, \Psi_c) \in Y^{\text{base}}$ with

$$Y^{\text{base}} := \mathbb{R}_+ \times \mathbb{R}_+ \times \mathbb{R}.$$

We can then compute unique coefficients for the higher order terms. We refer to these expansions as base expansions. For our numerical work we will use a base expansion

up to 7th order since higher order approximations do not yield improved results. Denote by $Y_\mu^{\text{base}} \subseteq Y^{\text{base}}$ the maximal domain for which these base coefficients are defined. We have that

$$Y_\mu^{\text{base}} = Y^{\text{base}}. \tag{18}$$

The derivation of Y_μ^{base} and higher order coefficients are presented in Appendix V-B.

The base expansion gives strong evidence that solutions $x_\mu(\cdot; \mu)$ satisfying T4 and

$$\begin{aligned} \lim_{s \rightarrow \infty} \Psi(s; \mu) - \frac{r_\infty h_\infty}{2} s &= \Psi_c, \\ \lim_{s \rightarrow \infty} z(s; \mu) - s &= 0, \end{aligned}$$

can be parameterized by $(r_\infty, h_\infty, \Psi_c) \in Y_\mu^{\text{base}}$.

D. CONNECTING TIP SOLUTIONS TO THE BASE EXPANSION

Consider the numerically computed $x_{\alpha_*}(\cdot; \mu)$ with $\alpha_* \in X_\mu$. Let s_1 be given by (11). Then, the numerics suggests that we can find a $s_0 < s_1$ such that $\rho'(s_0) \ll 1$ and $s_1 - s_0 \ll 1$. At $s = s_0$ we connect the r, h, Ψ, z -variables of the tip solution to the corresponding variables of the base expansion using a Newton method. Observe that we have four equations and that the base expansion has four degrees of freedom, three parameters given by $r_\infty, h_\infty, \Psi_c$ and one independent variable given by s . Note that the dependent variable s can be used as a degree of freedom in the base expansion since the governing ODE (4) is autonomous. The Newton method requires an initial vector. We have good estimates for r_∞, h_∞ since generally at $s = s_0$ the tip solution is close to the base. We do not have good estimates for Ψ_c and s . Hence, we continuously vary over initial estimates of these parameters until the tip solution smoothly connects to the base expansion.

IV. NUMERICAL RESULTS: BIFURCATION DIAGRAMS AND STEADY TIP GROWTH SOLUTIONS

We applied the numerical method to

$$\mu_i(\Psi) := 1 + \Psi^i, \quad \hat{\mu}_i(\Psi) := \Psi^i, \quad i = 2, 3, 4, 5. \tag{19}$$

Observe that $\mu_i, \hat{\mu}_i \in F$ where F is given by (6), $\mu_i, \hat{\mu}_i$ is analytic as required by Section III-A and $\nu_{\mu_i}, \nu_{\hat{\mu}_i}$, defined in (15), is analytic as required by Section III-C. We computed the tip solutions and classified these tip solution using the set A_μ and B_μ from (12). This yields a bifurcation diagram of the tip solutions corresponding to a given μ . For the viscosity function for which steady tip growth solutions exist we used the connection method of Section III-D.

A. VISCOSITY FUNCTIONS ADMITTING STEADY TIP GROWTH SOLUTIONS

The numerics suggests that the viscosity functions μ_3, μ_4, μ_5 admit steady tip growth solutions.

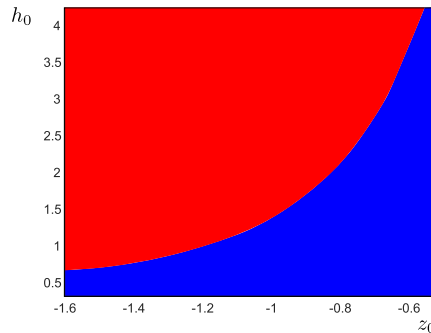


FIGURE 7. A_{μ_3} in blue and B_{μ_3} in red.

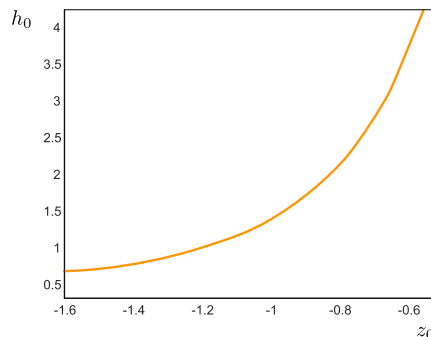


FIGURE 8. X_{μ_3} in orange.

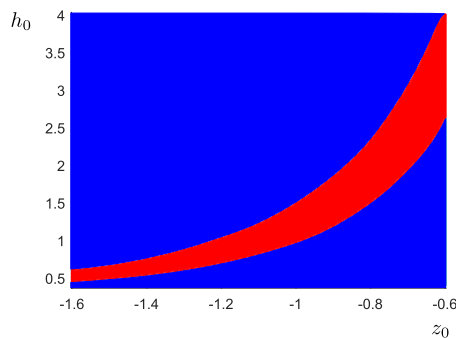


FIGURE 9. A_{μ_4} in blue and B_{μ_4} in red.

1) THE SET Y_μ^{tip}

Using (10) we compute $Y_{\mu_3}^{\text{tip}}, Y_{\mu_4}^{\text{tip}}, Y_{\mu_5}^{\text{tip}}$:

$$\begin{aligned} Y_{\mu_3}^{\text{tip}} &= \{(h_0, z_0) \in \mathbb{R}_+ \times \mathbb{R}_-\}, \\ Y_{\mu_4}^{\text{tip}} &= \{(h_0, z_0) \in \mathbb{R}_+ \times \mathbb{R}_- : h_0^4 z_0^8 \neq 5\}, \\ Y_{\mu_5}^{\text{tip}} &= \{(h_0, z_0) \in \mathbb{R}_+ \times \mathbb{R}_- : h_0^5 z_0^{10} \neq 2\}. \end{aligned}$$

2) BIFURCATION DIAGRAMS AND X_μ

In Fig. 7 we show the computed A_{μ_3} and B_{μ_3} . Fig. 7 suggests that A_{μ_3} and B_{μ_3} are connected sets. Then, if A_{μ_3} and B_{μ_3} are open then Fig. 7 suggests that $X_{\mu_3} \neq \emptyset$. In Fig. 8 we have computed X_{μ_3} .

In Fig. 9 and Fig. 10 we present the computed A_{μ_4}, B_{μ_4} and A_{μ_5}, B_{μ_5} , respectively. Fig. 9 and Fig. 10 suggest that B_{μ_4}, B_{μ_5} are connected sets and that A_{μ_4}, A_{μ_4} are

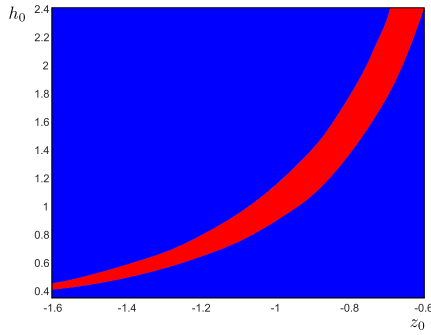


FIGURE 10. A_{μ_5} in blue and B_{μ_5} in red.

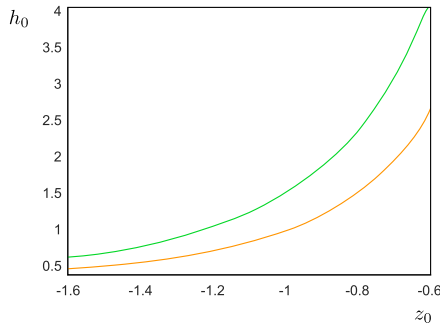


FIGURE 11. X_{μ_4} in orange and $h_0^A z_0^8 = 5$ in green.

disconnected sets consisting out of two connected components. If A_{μ_4}, B_{μ_4} and A_{μ_5}, B_{μ_5} are open the numerics also suggests that $X_{\mu_4} \neq \emptyset$ and $X_{\mu_5} \neq \emptyset$, respectively. In Fig. 11 and Fig. 12 we display by an orange curve the approximation

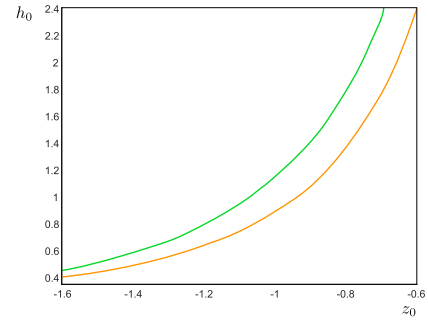


FIGURE 12. X_{μ_5} in orange and $h_0^5 z_0^{10} = 2$ in green.

of X_{μ_4} and X_{μ_5} , respectively. The green curve in Fig. 11 and Fig. 12 corresponds to the (h_0, z_0) which are not in $Y_{\mu_4}^{\text{tip}}$ and $Y_{\mu_5}^{\text{tip}}$, respectively. Hence, the green curve corresponds to the limiting values for which tip solutions do not exist.

Fig. 8, 11, 12 suggest that the parameter set corresponding to steady tip growth solutions is one dimensional. This means that almost all perturbations on X_{μ_i} are in $A_{\mu_i} \cup B_{\mu_i}$ where $i = 3, 4, 5$. Hence, steady tip growth solutions cannot be approximated by continuing tip solutions in forward s .

3) STEADY TIP GROWTH SOLUTIONS

In this section we will see that the numerical results suggest that steady tip growth solutions for μ_3, μ_4, μ_5 exist and that they correspond to tip solutions with parameters in $X_{\mu_3}, X_{\mu_4}, X_{\mu_5}$, respectively.

The range of steady tip growth solutions corresponding to μ_3, μ_4, μ_5 varies greatly. Hence, we scale each steady tip

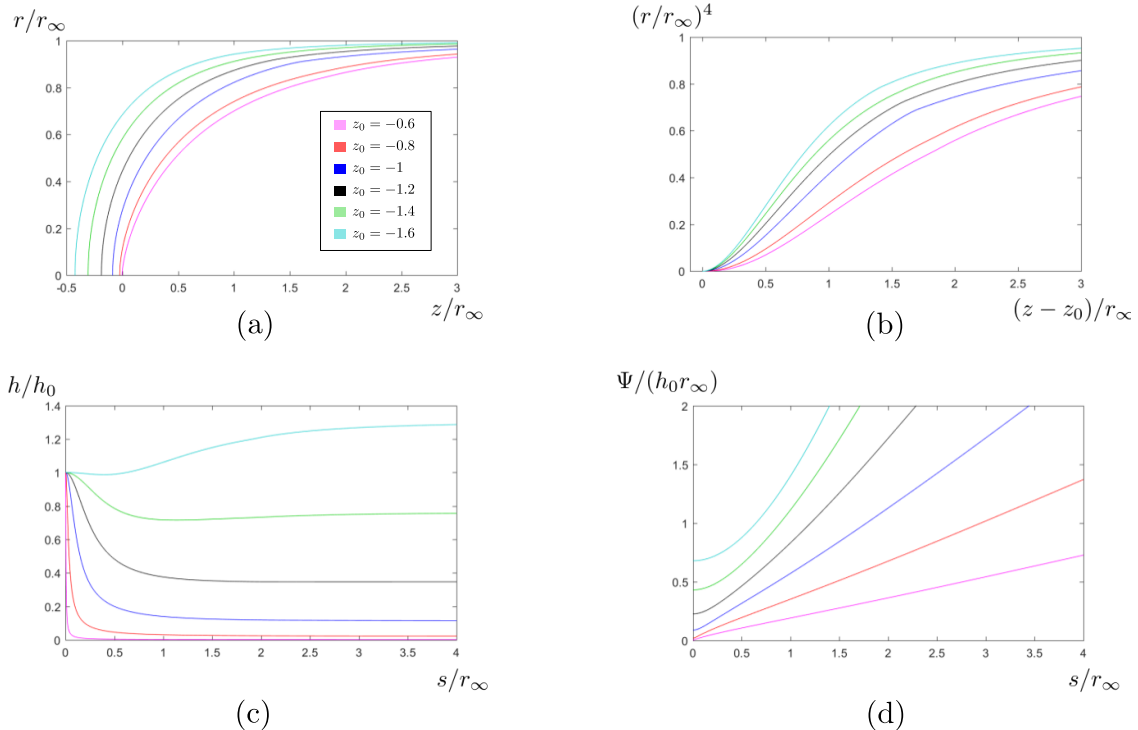


FIGURE 13. Steady tip growth solutions for μ_3 .

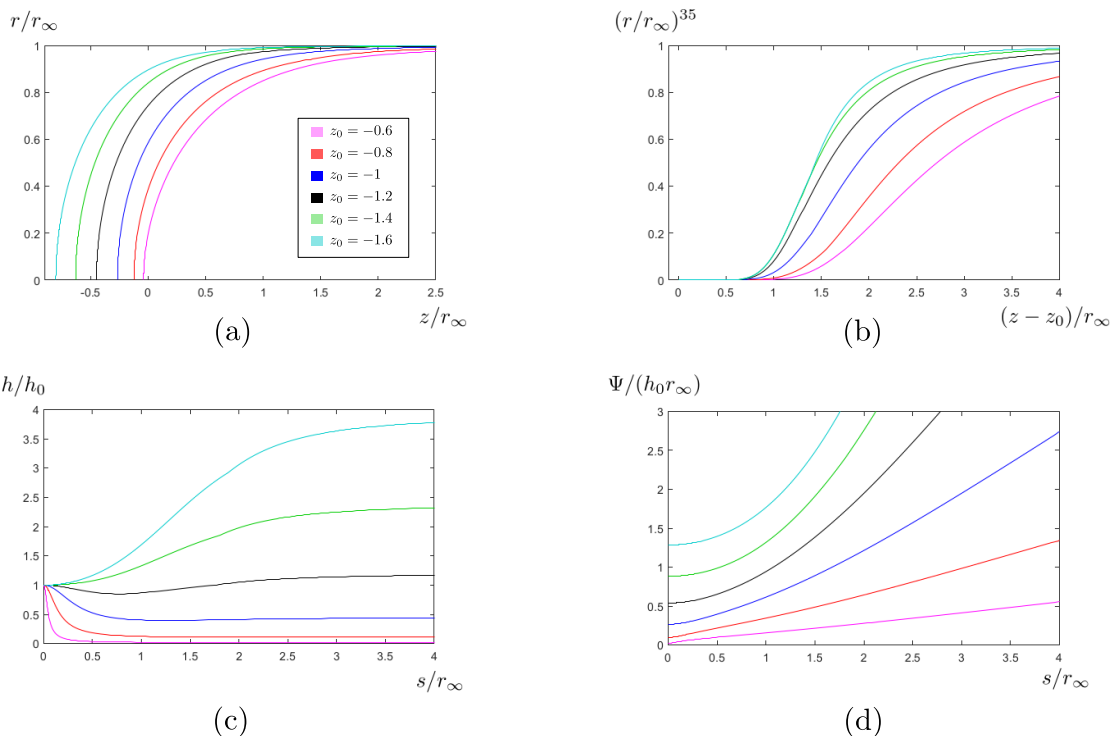


FIGURE 14. Steady tip growth solutions for μ_4 .

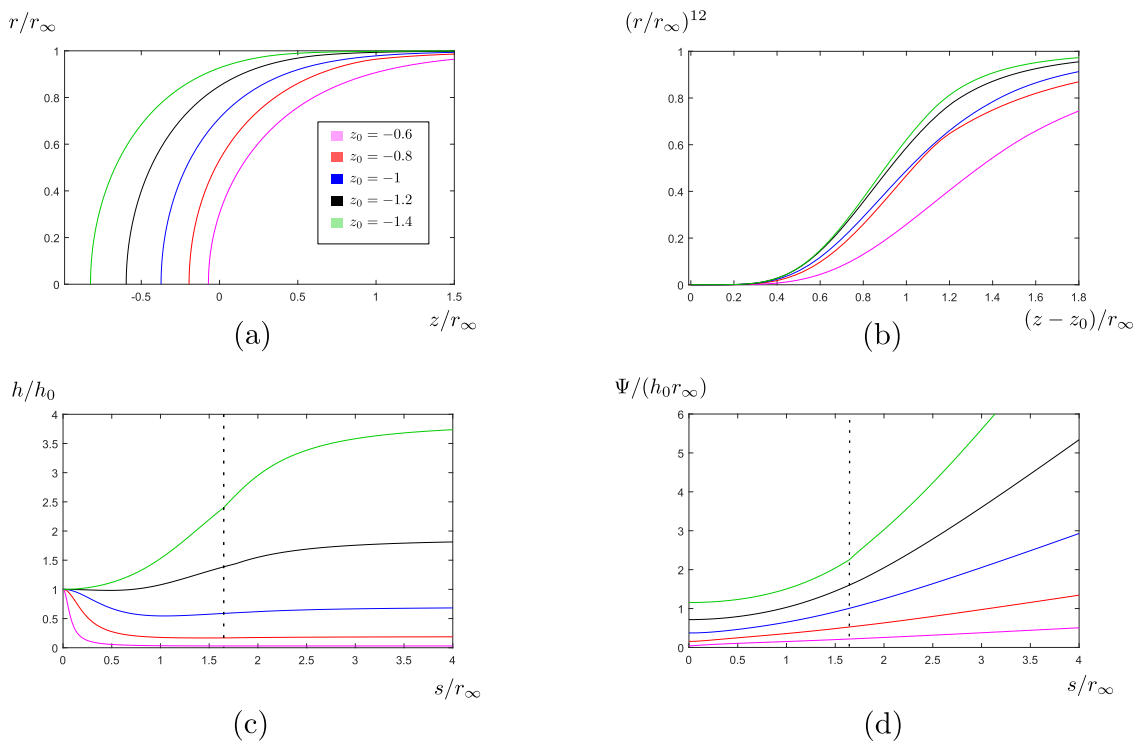


FIGURE 15. Steady tip growth solutions for μ_5 .

growth solution by its tip and base parameters. For visualization purposes we plot graphs for the rescaled variables: $r/r_\infty, z/r_\infty, h/h_0, \Psi/(h_0 r_\infty), s/r_\infty$.

In Fig. 13, 14, 15 we present the numerical approximations of tip solutions corresponding to parameters in $X_{\mu_3}, X_{\mu_4}, X_{\mu_5}$,

respectively. Fig. 13-15acd suggest that these tip solutions are steady tip growth solutions. Fig. 13-15acd suggest that the graphs of the corresponding scaled variables are ordered.

The numerically computed steady tip growth solutions are smooth with the exception of the steady tip growth

solution corresponding to $z_0 = -1.4$ as Fig. 15d shows. This non-smooth point occurs at the arclength s where the approximated tip solutions connects to the base expansion. Hence, denote the arclength at the connection point by s_{base} . This non-smoothness at $s = s_{\text{base}}$ worsens when z_0 is further decreased. Hence, we did not approximate steady tip growth solutions for $z_0 < -1.4$. For $z_0 = -1.4$ we observe that $h'(s_{\text{base}})$ is not small, see the dashed line in Fig. 15c. For the base expansion corresponding to μ_5 we have that $|h'(s)| \ll 1$ for s large. Hence, we expect that at $s = s_{\text{base}}$ the computed tip solution is not in the domain where the base expansion gives a good approximation of the steady tip growth solution. From Fig. 10 we observe that $(h_0, z_0) \in X_{\mu_5}$ with $z_0 \leq -1.4$ is close to the curve where the tip asymptotic expansion is not defined, $h_0^5 z_0^{10} = 2$. This might lead to an approximation of $(h_0, z_0) \in X_{\mu_5}$ with insufficient decimal precision which results in the non-smooth connection.

In Fig. 13b-15b we performed a transformation on the r -axis and z -axis to indicate that the tip shape of the scaled variables becomes more pointed when z_0 is increased. All these graphs are ordered.

Fig. 13-15d suggests that $\Psi' > 0$. Fig. 13d-15d suggests that h can be monotonously increasing, decreasing or have a local minimum.

B. VISCOSITY FUNCTIONS ADMITTING NO STEADY TIP GROWTH SOLUTIONS

For the $\mu_2, \hat{\mu}_2, \hat{\mu}_3, \hat{\mu}_4, \hat{\mu}_5$ the tip expansions are defined for all $(h_0, z_0) \in \mathbb{R}_+ \times \mathbb{R}_-$.

The numerical work suggests that $\mu_2, \hat{\mu}_2, \hat{\mu}_3, \hat{\mu}_4, \hat{\mu}_5$ admit no steady tip growth solutions. More specifically, it suggests that

$$A_{\mu_2} = A_{\hat{\mu}_2} = A_{\hat{\mu}_4} = A_{\hat{\mu}_5} = B_{\hat{\mu}_3} = \mathbb{R}_+ \times \mathbb{R}_-$$

Furthermore, we observe that the computed tip solutions corresponding to $\mu_2, \hat{\mu}_2, \hat{\mu}_4, \hat{\mu}_5$ satisfy $\Psi' < 0$ and that the computed tip solutions corresponding to $\hat{\mu}_3$ satisfy $\Psi' > 0$. These observations are also supported by the sign of the leading order term corresponding to the tip expansion of Ψ' .

V. CONCLUSION AND FUTURE WORK

Fungal filaments occur in pathogenic and symbiotic fungi. Hence, it is relevant to study fungal growth models such as the BATS model. We give an overview of the obtained results and discuss future research directions.

A. OVERVIEW RESULTS

Our numerical results suggest that there exist viscosity functions for which steady tip growth solutions exist. Hence, we have evidence which supports the BATS model. Furthermore, there exist viscosity functions for which steady tip growth solutions do not exist. This suggests that the viscosity function is a determining factor for tip growth in the BATS model.

The bifurcation diagrams suggests that if there exists a steady tip growth solution then there also exists a one

parameter family of steady tip growth solutions. In relation to the cell shape this parameter influences the pointedness of the cell's tip. Hence, the BATS model allows for a variety of different cell shapes.

B. FUTURE RESEARCH DIRECTIONS

From a mathematical perspective it would be interesting to rigorously prove the existence of steady tip growth solutions. The numerical work suggests that the set A_μ, B_μ can be helpful in proving the existence of steady tip growth solutions. The governing ODE (4) is a five dimensional first order ODE. Hence, it might be fruitful to create a toy model with solutions corresponding to A_μ, B_μ and then show that these sets can be used to prove the existence of a toy steady tip growth solutions.

The computed bifurcation diagrams suggest that if $x(\cdot; \mu)$ is a steady tip growth solution then h_0 or z_0 as given by condition T1 defines a unique steady tip growth solution. Hence, to compute the steady tip growth solution we only need to have data on μ and on either h_0 or z_0 . It is important to observe that the governing ODE (4) is non-dimensionalised. During non-dimensionalisation the cell's parameters have been absorbed in the viscosity function [12]. These parameters concern the pressure difference between the inside and outside of the cell and the rate of cell-wall building material emitted by the VSC, see Fig. 2. Consequently, experiments need to be performed to obtain these parameters.

The numerical method can be applied to validate the BATS model in an experimental setting. However, a method to process the data is still needed. The data processing method should be able to compute a viscosity function which fits the experimental data. Then, in combination with biological parameters it should be possible to verify the BATS model using the presented numerical method. The authors are unaware if the required biological experiments have been performed. Once this data has been obtained a data processing method can be implemented.

In conclusion, we have formulated a numerical technique such that the BATS model can be validated by a to be developed data driven methodology.

APPENDIX A EXPANSIONS

We present coefficients of the variables r, h, Ψ, z for the expansions at the tip and the base. The coefficients corresponding to ρ are not presented since they can be directly obtained using $r' = \rho$ from the governing ODE (4).

The expressions become lengthy for high order coefficients. Hence, we only present low order coefficients. These coefficients were computed symbolically using Mathematica (TM). The script is available on request.

A. TIP EXPANSION

Let $x(\cdot; \mu)$ be a tip expansion as defined in Section III-A. The viscosity function μ is analytic. We denote the i -th coefficient of the formal expansion of μ by an (i) superscript. Recall from Section III-A that r is an odd function. We present the 1st and

3rd order coefficients of r :

$$r_{\text{tip}}^{(1)} = 1,$$

$$r_{\text{tip}}^{(3)} = -\frac{2z_0^4}{27\mu(h_0z_0^2)^2}.$$

Recall from Section III-A that h, Ψ, z are even functions. We present the 2nd order coefficients of h, Ψ, z :

$$h_{\text{tip}}^{(2)} = h_0(-4h_0z_0^8\mu'(h_0z_0^2) + 8z_0^5\mu(h_0z_0^2)(z_0 - 3h_0\mu'(h_0z_0^2)) + z_0^2\mu(h_0z_0^2)^2(64z_0 - 27h_0\mu'(h_0z_0^2)) + 72\mu(h_0z_0^2)^3) \times (6z_0^2\mu(h_0z_0^2)^2(3h_0z_0^2\mu'(h_0z_0^2) - 10\mu(h_0z_0^2)))^{-1},$$

$$\Psi_{\text{tip}}^{(2)} = \frac{h_0(24z_0^3\mu(h_0z_0^2) + 27\mu(h_0z_0^2)^2 + 8z_0^6)}{18\mu(h_0z_0^2)(10\mu(h_0z_0^2) - 3h_0z_0^2\mu'(h_0z_0^2))},$$

$$z_{\text{tip}}^{(2)} = \frac{z_0^2}{3\mu(h_0z_0^2)}.$$

The lower order coefficients for r, h, Ψ, z are given in Section III-A. Observe that the denominator in the expression for $h_{\text{tip}}^{(2)}$ and $\Psi_{\text{tip}}^{(2)}$ is zero for

$$\frac{10}{3} = \frac{h_0z_0^2\mu'(h_0z_0^2)}{\mu(h_0z_0^2)}.$$

More generally, the tip coefficients are defined if and only if $(h_0, z_0) \in Y_{\mu}^{\text{tip}}$.

B. BASE EXPANSION

Let $x(\cdot; \mu)$ be a base expansion as defined in Section III-C. We fix $z_c = 0$ since we showed in Section III-C that the z_c parameter can be absorbed in the independent variable s . The function v_{μ} defined in (16) is assumed to be analytic. We denote the i -th coefficient of the formal expansion of v_{μ} by an (i) superscript. Since $\mu \in F$ with F given by (6) we have that $v_{\mu}^{(0)} = 0$. As a result of Appendix VI we assume that $v_{\mu}(\psi) \in O(\psi^2)$ for $\psi \rightarrow 0$. Hence, we have that $v_{\mu}^{(1)} = 0$. The 1st and 2nd order coefficients for r, h, Ψ are given by

$$r_{\text{base}}^{(1)} = -\frac{2v_{\mu}^{(2)}r_{\infty}}{h_{\infty}^2},$$

$$r_{\text{base}}^{(2)} = \frac{4v_{\mu}^{(2)}\Psi_ch_{\infty} - 2v_{\mu}^{(3)}h_{\infty} + 6(v_{\mu}^{(2)})^2r_{\infty}}{h_{\infty}^4},$$

$$h_{\text{base}}^{(1)} = \frac{2v_{\mu}^{(2)}}{h_{\infty}},$$

$$h_{\text{base}}^{(2)} = -\frac{16v_{\mu}^{(2)}\Psi_ch_{\infty} - 8v_{\mu}^{(3)}h_{\infty} + h_{\infty}^4r_{\infty}^3 + 8(v_{\mu}^{(2)})^2r_{\infty}}{4h_{\infty}^3r_{\infty}},$$

$$\Psi_{\text{base}}^{(1)} = \frac{1}{4}h_{\infty}r_{\infty}^3,$$

$$\Psi_{\text{base}}^{(2)} = -\frac{r_{\infty}^2(-2\Psi_ch_{\infty} + 6v_{\mu}^{(2)}r_{\infty})}{8h_{\infty}}.$$

For z we have that $z_{\text{base}}^{(1)} = z_{\text{base}}^{(2)} = 0$. The 3rd and 4th order coefficients for z are given by

$$z_{\text{base}}^{(3)} = \frac{2(v_{\mu}^{(2)})^2r_{\infty}^2}{3h_{\infty}^4},$$

$$z_{\text{base}}^{(4)} = -\frac{v_{\mu}^{(2)}r_{\infty}(4v_{\mu}^{(2)}\Psi_ch_{\infty} - 2v_{\mu}^{(3)}h_{\infty} + 6(v_{\mu}^{(2)})^2r_{\infty})}{h_{\infty}^6}.$$

The lower order coefficients of the base expansion are presented in Section III-C. Observe that the base coefficients are defined for all $(r_{\infty}, h_{\infty}, \Psi_c) \in Y_{\mu}^{\text{base}}$.

VI. NECESSARY CONDITION VISCOSITY FUNCTION FOR SOLUTIONS SATISFYING T4

Recall v_{μ} defined in (16). We will show that if $v_{\mu}(\psi) \sim c_1\psi$ for $\psi \rightarrow 0$ with $c_1 > 0$ then the governing ODE (4) does not have solutions satisfying T4. Observe that by (16) it follows that $v_{\mu}(\psi) \sim c_1\psi$ for $\psi \rightarrow 0$ is equivalent to

$$\mu(\Psi) \sim \frac{1}{c_1\Psi} \text{ for } \Psi \rightarrow \infty. \quad (20)$$

Assume that x is a solution satisfying T4. Then for $s \rightarrow \infty$ we have that

$$\frac{r(s)\gamma(\rho(s), r(s), z(s))}{\Gamma(r(s), z(s))} \sim \frac{c_2}{s^3},$$

$$\frac{r(s)^2}{2\mu(\Psi(s))\Gamma(r(s), z(s))\sqrt{1-\rho(s)^2}} \sim \frac{c_3}{s}, \quad (21)$$

where $c_2, c_3 > 0$. We can re-write the h -equation in the ODE (4) as

$$\frac{(h\sqrt{r})'}{h\sqrt{r}} = \frac{r\gamma(\rho, r, z)}{\Gamma(r, z)} - \frac{r^2}{2\mu(\Psi)\Gamma(r, z)\sqrt{1-\rho^2}}. \quad (22)$$

Using (21) in equation (22) we find that there exist s_1 and $c_4 > 0$ such that

$$\frac{(h(s)\sqrt{r(s)})'}{h(s)\sqrt{r(s)}} \leq -\frac{c_4}{s} \text{ for all } s > s_1.$$

Integration yields that $\lim_{s \rightarrow \infty} h(s) = 0$ which is in contradiction with the h -limit given in condition T4.

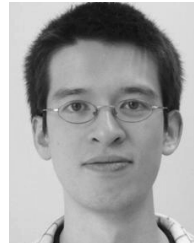
ACKNOWLEDGMENT

T. G. de Jong was with the Center for Analysis, Scientific Computing and Applications (CASA), TU Eindhoven, 5612 AZ Eindhoven, The Netherlands.

REFERENCES

- [1] S. Bartnicki-Garcia, C. E. Bracker, G. Gierz, R. López-Franco, and H. Lu, "Mapping the growth of fungal hyphae: Orthogonal cell wall expansion during tip growth and the role of turgor," *Biophys. J.*, vol. 79, no. 5, pp. 2382–2390, 2000.
- [2] S. Bartnicki-Garcia and G. Gierz, "A three-dimensional model of fungal morphogenesis based on the vesicle supply center concept," *J. Theor. Biol.*, vol. 208, pp. 151–164, Jan. 2001.
- [3] S. Bartnicki-Garcia, F. Hergert, and G. Gierz, "Computer simulation of fungal morphogenesis and the mathematical basis for hyphal (tip) growth," *Protoplasma*, vol. 153, nos. 1–2, pp. 46–57, 1989.
- [4] O. Campàs and L. Mahadevan, "Shape and dynamics of tip-growing cells," *Current Biol.*, vol. 19, no. 24, pp. 2102–2107, 2009.

- [5] A. Chowdhary, K. Agarwal, and J. F. Meis, "Filamentous fungi in respiratory infections. What lies beyond Aspergillosis and Mucormycosis?" *PLoS Pathogen*, vol. 12, no. 4, 2016, Art. no. e1005491.
- [6] R. A. Cole and J. E. Fowler, "Polarized growth: Maintaining focus on the tip," *Current Opinion Plant Biol.*, vol. 9, no. 6, pp. 579–588, 2006.
- [7] E. Eggen, M. N. de Keijzer, and B. M. Mulder, "Self-regulation in tip-growth: The role of cell wall ageing," *J. Theor. Biol.*, vol. 283, no. 1, pp. 113–121, 2011.
- [8] A. Goriely, *The Mathematics and Mechanics of Biological Growth* (Interdisciplinary Applied Mathematics), vol. 45. New York, NY, USA: Springer, 2017.
- [9] A. Goriely, M. Tabor, and A. Tongen, "A morpho-elastic model of hyphal tip growth in filamentous organisms," in *Proc. IUTAM Symp. Cellular, Mol. Tissue Mech.*, K. Garikipati and E. Arrudar, Eds. Dordrecht, The Netherlands: Springer, 2004, pp. 232–260.
- [10] F. M. Harold, "Force and compliance: Rethinking morphogenesis in walled cells," *Fungal Genet. Biol.*, vol. 37, no. 3, pp. 271–282, 2002.
- [11] T. de Jong, "Topological shooting, invariant manifold theory and rigorous numerics applied to an ODE for hypha tip growth," Ph.D. dissertation, Eindhoven Univ. Technol., Eindhoven, The Netherlands, 2019.
- [12] T. de Jong, G. Prokert, and J. Hulshof. (2019). "Modeling fungal hypha tip growth via viscous sheet approximation." [Online]. Available: <https://arxiv.org/abs/1903.03565>
- [13] T. de Jong, G. Prokert, and J. Hulshof, "A new model for fungal hyphae growth using the thin viscous sheet equations," in *Proc. Int. Conf. Comfos*, 2016, pp. 175–184.
- [14] M. N. de Keijzer, A. M. Emons, and B. M. Mulder, "Modeling tip growth: Pushing ahead," in *Root Hairs*, T. Ketelaar and A. M. Emons, Eds. Berlin, Germany: Springer, 2009, pp. 103–122.
- [15] A. L. Koch, "The problem of hyphal growth in streptomycetes and fungi," *J. Theor. Biol.*, vol. 171, pp. 137–150, Nov. 1994.
- [16] U. Kück, S. Bloemendaal, and I. Teichert, "Putting fungi to work: Harvesting a cornucopia of drugs, toxins, and antibiotics," *PLoS Pathogens*, vol. 10, no. 3, 2014, Art. no. e1003950.
- [17] N. P. Money, "Insights on the mechanics of hyphal growth," *Fungal Biol. Rev.*, vol. 22, no. 2, pp. 71–76, 2008.
- [18] D. R. Olicón-Hernández, J. González-López, and E. Aranda, "Overview on the biochemical potential of filamentous fungi to degrade pharmaceutical compounds," *Frontiers Microbiol.*, vol. 8, p. 1792, Sep. 2017.
- [19] G. Steinberg, "Hyphal growth: A story of motors, lipids, and the spitzenkörper," *Eukaryotic Cell*, vol. 6, no. 3, pp. 351–360, 2007.
- [20] S. H. Tindemans, N. Kern, and B. M. Mulder, "The diffusive vesicle supply center model for tip growth in fungal hyphae," *J. Theor. Biol.*, vol. 238, no. 4, pp. 937–948, 2006.



THOMAS G. DE JONG was born in Groningen, The Netherlands, in 1987. He received the M.S. degree in mathematics from the University of Groningen, The Netherlands, in 2012, and the Ph.D. degree in mathematics from the Eindhoven University of Technology, in 2019.

His research interests include nonlinear dynamical systems, biomathematics, celestial mechanics, and machine learning.

Dr. de Jong's awards and honors include the ICI-ECP Scholarship, the JASSO Scholarship, the Nonlinear Dynamics of Natural Systems Best Poster Presentation, and the Equadiff Best Post Award. His doctoral project was partly supported by the Dutch Mathematics Cluster Nonlinear Dynamics of Natural Systems and a Vici grant.



ALEF E. STERK was born in Sneek, The Netherlands, in 1982. He received the M.S. and Ph.D. degrees in mathematics from the University of Groningen, The Netherlands, in 2006 and 2010, respectively.

From 2010 to 2012, he was an Associate Research Fellow with the University of Exeter, U.K. From 2012 to 2013, he was a Lecturer with the University of Twente. Since 2014, he has been an Assistant Professor with the Bernoulli Institute,

University of Groningen. His research interests include nonlinear dynamical systems, and the mathematical analysis of models in climate and biology.

Dr. Sterk is a member of the Dutch Mathematics Cluster Nonlinear Dynamics of Natural Systems and the Dutch network Mathematics of Planet Earth, which are both supported by the Netherlands Organisation for Scientific Research.



FENG GUO was born in Fuzhou, China, in 1979. He received the M.S. and Ph.D. degrees in computer science from Xiamen University, China, in 2005 and 2011, respectively.

His research interests include augmented reality, computer vision, and machine learning.

Dr. Guo is currently an Assistant Professor with the School of Information Science and Engineering, Xiamen University. He is also the Deputy Secretary General of the Artificial Intelligence Society of Fujian Province, China.

• • •